Proceedings of the 12th International Conference on Heat Transfer and Fluid Flow (HTFF 2025)

Paris, France - August, 2025 Paper No. HTFF 169 DOI: 10.11159/htff25.169

Investigation of Airflow in Human Nasal Cavity and Virtual Septoplasty Using CFD

Cem Turutoglu¹, Sertac Cadirci²

¹Istanbul Technical University, Department of Mechanical Engineering 34437, Istanbul, Türkiye turutoglu16@itu.edu.tr

²Istanbul Technical University, Department of Mechanical Engineering 34437, Istanbul, Türkiye cadircis@itu.edu.tr

Abstract - Breathing is essential for oxygen supply, and nasal structure significantly impacts airflow. Conditions like septal deviation which affect 20-35% of people often require septoplasty, but long-term outcomes remain uncertain. Virtual surgery, combining CFD and medical imaging, offers a predictive tool to evaluate surgical efficacy beforehand. This study presents a CFD simulation of airflow in human nasal cavity and proposes a numerical methodology for virtual septoplasty. The method was validated using the Carleton University Standardized Human Nasal Cavity Geometry available in the open-source literature. Virtual septoplasty was simulated by modifying computational grid of the nasal cavity, and pre-/postoperative flow results were compared at various breath rates. Key parameters involving nasal resistance and nasal power were quantified. Results demonstrated measurable changes in airflow dynamics, enabling objective assessment of surgical outcomes. This approach helps clinicians predict postoperative improvements, avoid unnecessary surgeries, and enhance patient counselling. The study highlights the potential of the interdisciplinary collaboration of engineers and medical doctors in surgical planning.

Keywords: Computational Fluid Dynamics (CFD), nasal airflow, virtual surgery, septoplasty

1. Introduction

Although medical research on nasal anatomy dates back to the late 19th century [1], studies on the nasal cavity in the field of bioengineering have emerged only in the last 70 years [2]. In bioengineering, numerical studies on the upper respiratory tract and nasal cavity have been conducted to understand the physics of airflow related to nasal physiology, analyze the distribution of particles (e.g., drugs or nasal sprays) within the nasal cavity, and evaluate surgical interventions in the context of virtual surgery planning.

Most Computational Fluid Dynamics (CFD)-based studies validate their results by comparing them with other experimental and numerical data in the literature. A major challenge in such comparisons is the anatomical variability of nasal cavities between individuals, making direct comparisons using one reference difficult. Consequently, researchers are compelled to compare the variation in cross-sectional areas along the flow path [3, 4]. Additionally, studies have evaluated velocity fields at various flow rates [4], calculated pressure drops resembling Moody diagrams through in-vitro experiments and CFD analyses [5], and calculated pressure drop and wall shear stress along the flow direction [6, 7, 8]. Some studies focus on determining nasal resistance, i.e. a measure of respiratory difficulty caused by physiological disorders, by correlating pressure drop with flow rate under different conditions. These investigations include numerical and experimental approaches, covering flow rates ranging from resting to active breathing states.

Septal deviation is one of the most common nasal disorders. On the other side, nasal obstructions, polyps, or tumors, can also impede airflow. Xu et al. [9] used CFD to calculate pressure drops affected by sleep apnea. Zhao et al. [7] numerically assessed the efficacy of mandibular advancement devices in sleep apnea patients by comparing pre- and post-treatment Computer Tomography (CT) scans. Mylavarapu et al. [10] employed virtual surgery to explore personalized treatments for tracheal stenosis. Flint et al. [11] investigated empty nose syndrome using CFD, where excessive turbinate removal leads to severe nasal pain. Jordal [12] studied pre- and post-operative nasal resistance in sleep apnea patients with obstructions, and Fan et al. [13] evaluated surgical outcomes by comparing CFD results from pre- and post-operative CT scans. Kita et al. [14]

compared pressure distributions in the anterior, middle, and posterior nasal sections before and after bimaxillary orthognathic surgery as an indicator of breathing quality. Kim et al. [15] numerically examined pre- and post-operative changes in septoplasty and upper airway obstruction cases by evaluating nasal resistance reduction, airflow partitioning between nostrils, local velocity maxima, and wall shear stress. They suggested CFD as a diagnostic tool for septal deviation. Garcia et al. [16] studied how obstruction location affects nasal resistance and proposed virtual septoplasty to identify high-benefit candidates for surgery. Xiong et al. [17] studied the impact of virtual functional endoscopic sinus surgery on airflow, highlighting the potential of CFD in preoperative planning. Ozlugedik et al. [18] assessed septal deviation and concha bullosa effects via 3D-CFD. Rhee et al. [19] compared virtual and actual septoplasty outcomes and found close agreement between them and emphasized the role of CFD in real-time surgical optimization. Liu et al. [20] studied the effects of airflow in septal deviation, and Chen et al. [21] used CFD to associate the pathological changes in the nasal cavity to physiological dysfunction, aiding surgeons in predicting aerodynamic outcomes. Such studies not only evaluate nasal pathologies but also enhance surgical success rates by forecasting intervention effects.

The current study aims to assist surgeons in predicting the benefits of septal deviation correction by modelling virtual surgery before the actual medical operation. A deviated septum was computationally generated by using the non-deviated Carleton-Civic [3] model, and CFD analyses were performed under identical boundary conditions. Nasal resistance and required breathing power were compared between the deviated and normal models, demonstrating the method's feasibility for patient-specific treatment.

2. Methodology

Inhaled air passes through the nasal cavity before reaching the trachea and lungs. Fig. 1 (a) shows a coronal section of the nasal cavity with labelled anatomical regions. Septal deviation, defined as the displacement of the nasal septum into either nasal passage, is a common condition affecting approximately 26% of healthy adults [15]. Consequently, septoplasty is frequently recommended for patients exhibiting elevated nasal resistance.

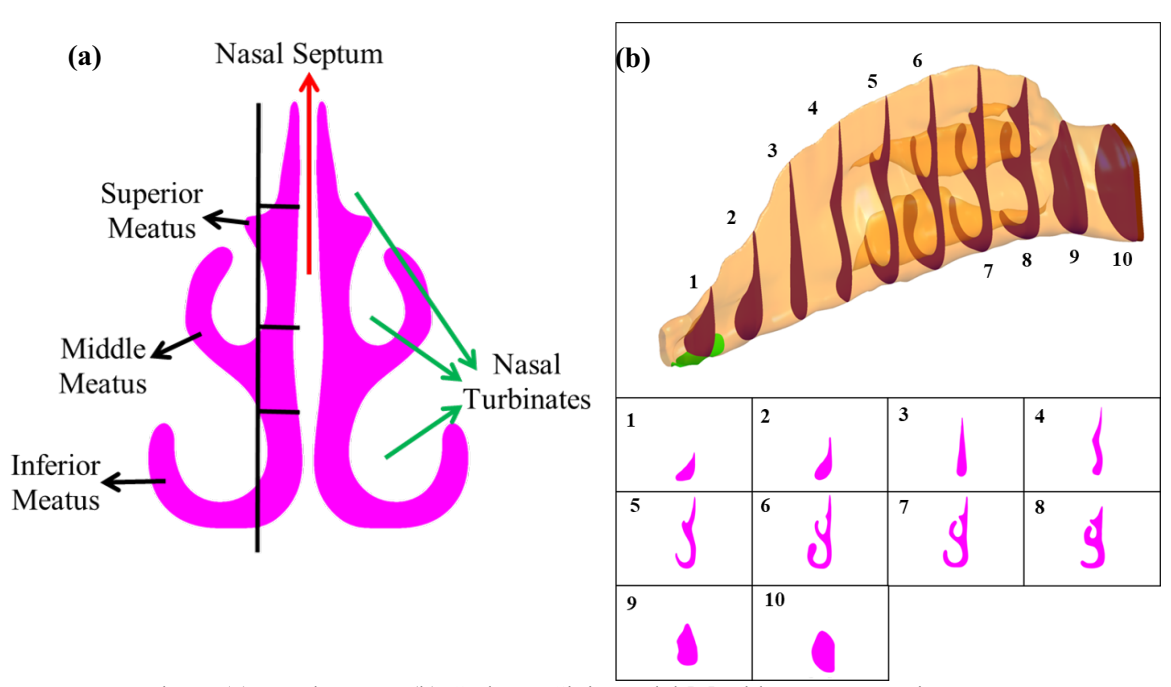


Fig. 1: (a) Nasal septum (b) Carleton-Civic model [3] with 10 cross-section area

Upper respiratory tract models are typically reconstructed from CT or Magnetic Resonance (MR) images. This study utilized the Carleton-Civic model, a standardized nasal cavity geometry derived from 30 individuals with non-deviated

septum. During inhalation, negative pressure generated by lung expansion, sucks air through the nostrils into the nasopharynx shown Fig. 1(b). Nasal resistance arises from the pressure loss and is calculated as the ratio of the trans-nasal pressure drop (ΔP) to the volumetric flow rate (Q) [21].

The flow dynamics within the nasal cavity is highly complex. To reduce computational cost and ease the simulations, several assumptions have been done: heat and mass transfer between the mucosa and air were neglected; microscopic particles and substructures were excluded; and no-slip boundary conditions were applied on the rigid walls of the nasal cavity. At the nostril, mass-flow-inlet boundary condition was employed representing plug-flow, while the outlet boundary condition was defined as zero-gauge pressure at nasopharynx. Air was treated as an incompressible gas with a constant density of 1.225 kg/m³ at standard atmospheric conditions.

Breathing involves bidirectional flow, mathematically represented by a sinusoidal cycle. To justify steady-state analysis, the Womersley number was computed as 1.48, for the breathing frequency of 1.57 Hz and a hydraulic diameter of 0.01 m. At a flow rate of 30 L/min, the Strouhal number (St) was calculated as 0.0035, confirming steady-state applicability (St<1). At this flow rate, the Reynolds number (Re) is approximately 2950, placing the flow in the transitional regime for internal duct flows [22]. As the turbulence model, the Transition SST model was assigned with an inlet turbulence intensity of 5% at the nostril. The governing RANS equations and turbulence transport models solved by Ansys®-Fluent can be found in reference [23].

Computational grid of the Carleton-Civic model was generated using ICEM-CFD[®]. To indicate the sufficient number of elements, mesh independence study was conducted. In this context, analyses were performed using five different grids, as tabulated in Table 1.

Table 1	: Number	of eleme	nt for diffe	rent meshes.

	Grid-1	Grid-2	Grid-3	Grid-4	Grid-5
Number of elements	954,017	1,586,652	2,431,075	3,283,024	4,593,420

These meshes were generated to keep wall y^+ values below 1. Special care was taken to ensure that the computational grid is compatible with the selected turbulence model and does not affect numerical stability. Thus, this mesh structure with low skewness and aspect ratio allowed for robust solutions with satisfactory convergence. The comparison of ΔP results versus the number of elements is presented in Fig. 2.

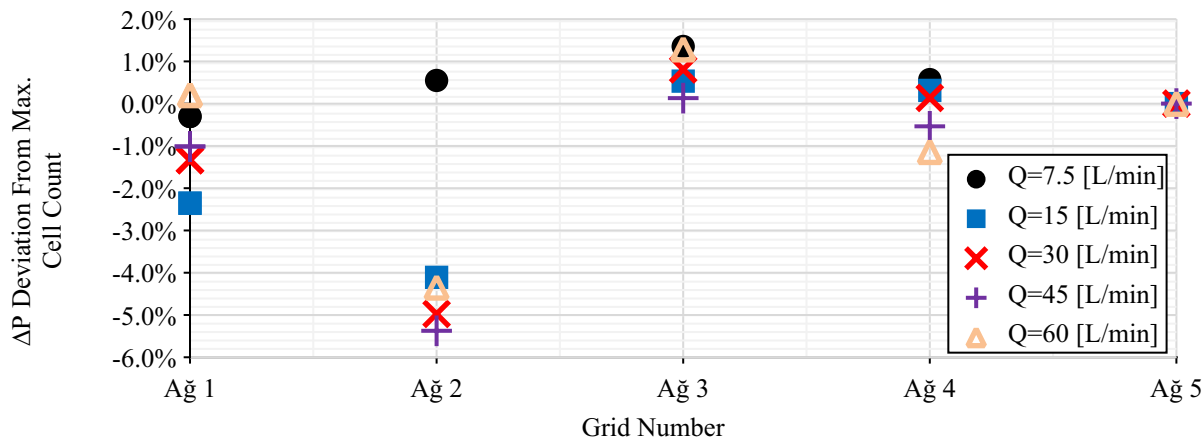


Fig. 2: ΔP variations for different grids

Figure 3(a) shows that Grid-5 was determined as the most suitable mesh configuration for this study. As shown in Fig. 3(b) and 3(c), inverse virtual septoplasty, performed on the non-deviated septum, was simulated by deforming the anterior-inferior region, i.e. the area most impactful on nasal resistance, following the methodologies proposed by Xiong et al. [17].

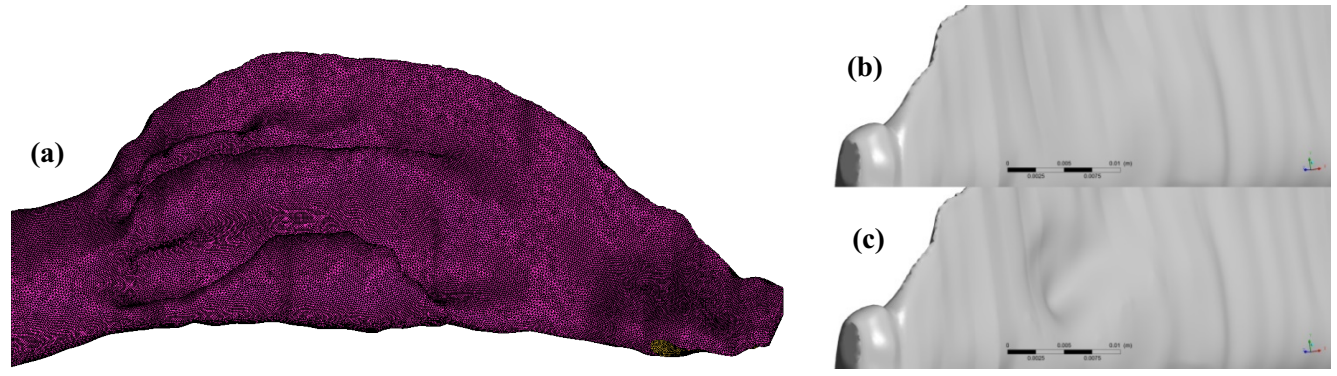


Fig. 3: (a) Selected grid (b) Carleton-Civic model (c) Carleton-Civic model with deviated septum

3. Results

The CFD results obtained for different flow rates were compared with the results reported by Liu et al. [24, 25] for the same model and with the experimental and numerical results obtained by Weinhold and Mlynski [26] for validation purposes. As shown in Fig. 4, the methodologies employed in this study show alignment with benchmark studies in the literature.

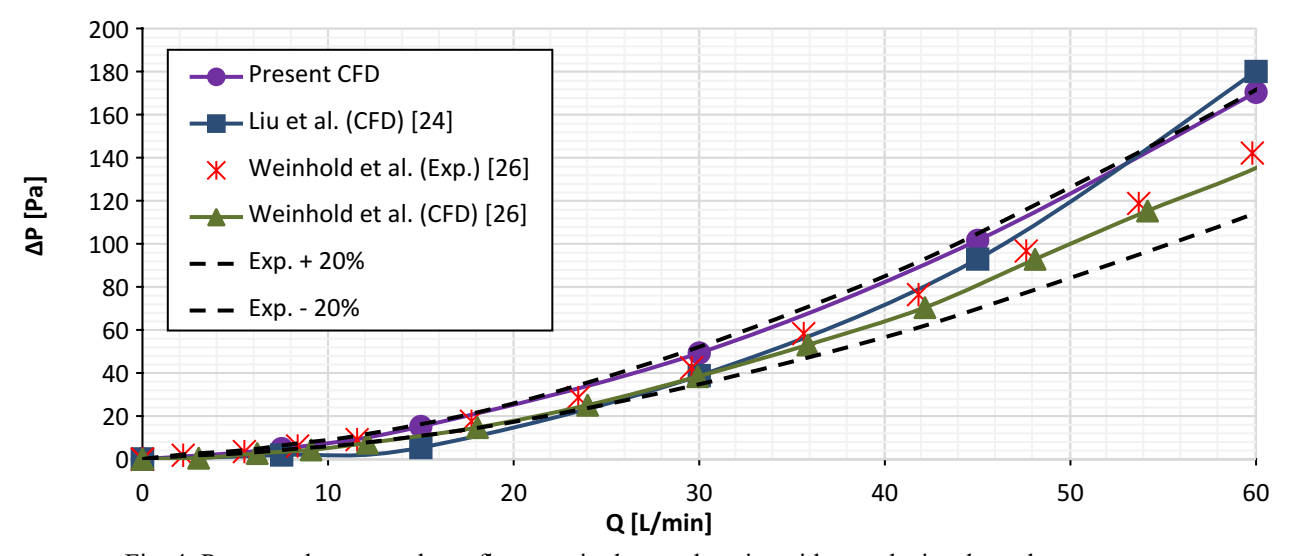


Fig. 4: Pressure drop vs. volume flow rate in the nasal cavity with non-deviated nasal septum

Following the validation process, CFD analyses were performed under the same boundary conditions on the deviated septum geometry created from the Carleton model. The resulting changes in nasal resistance and nasal power were calculated and tabulated in Table 2. According to Table 2, a volumetric contraction of approximately 1% within the nasal cavity leads to nearly 7-8% increase in nasal resistance, particularly under resting conditions at inhalation rates of 7.5 L/min and 15 L/min. These results indicate that an individual with septal deviation would expend about 8% more nasal power to maintain the same flow rate during rest. However, as the inhalation flow rate increases, the effect of septal deviation on nasal resistance and nasal power diminishes.

Table 2: The comparison of the CFD results for deviated and non-deviated nasal cavity.

	Flow Rate [L/min]	Nasal Resistance [kPa/(m³/s)]	Nasal Power P [mWatt]	Nasal Resistance Variation [%]	Nasal Power Variation [%]
Non- Deviated Model	7.5	39.4	0.615		
	15	60.3	3.769		
	30	101.6	25.412	_	
	45	138.6	77.972	_	
	60	173.8	173.764	_	
Deviated -	7.5	42.4	0.663	7.2	7.2
	15	65.8	4.114	8.4	8.4
	30	106.2	26.555	4.3	4.3
	45	142.3	80.081	2.6	2.6
	60	176.4	176.432	1.5	1.5

To better examine the differences between the non-deviated and deviated nasal cavity models at a flow rate of 30 L/min, velocity distributions across various sections were compared in Fig. 5. The effects of septal deviation were most pronounced in the second section, just before the region where the curvature is most prominent (cross-section 3). The highest velocity magnitude was observed in the deviated model, exceeding that of the non-deviated model. Beyond the deviated region, velocity distributions were notably lower.

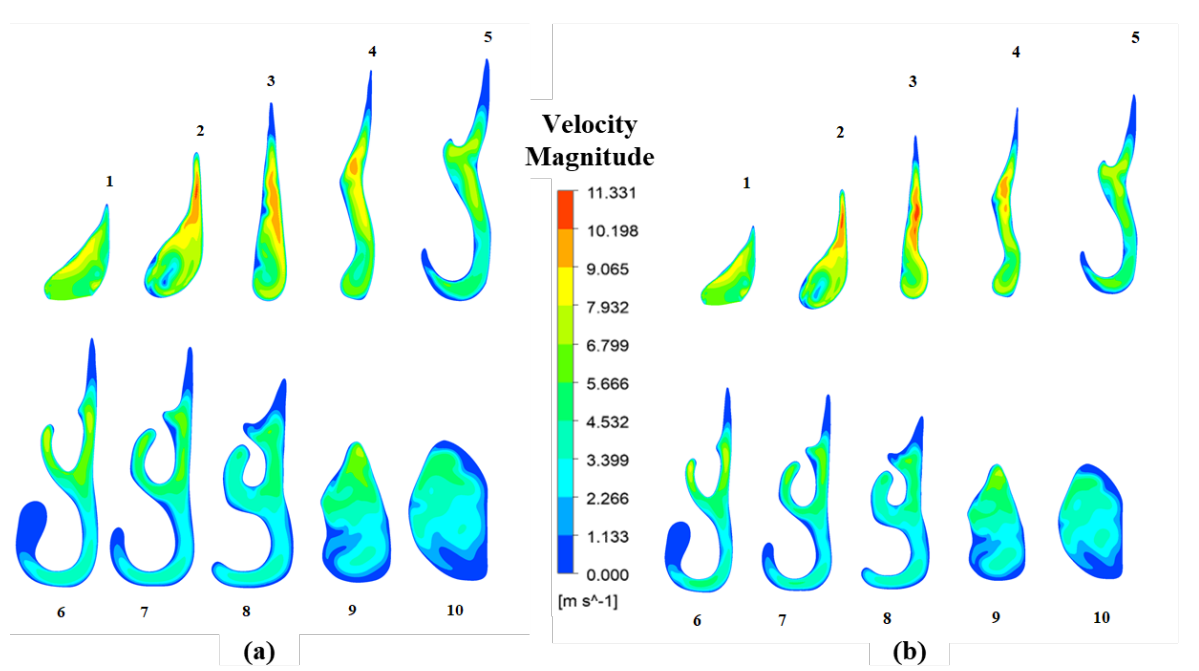


Fig. 5: Velocity distributions at each cross section at 30 L/min flow rate (a) non-deviated septum, (b) deviated septum

Similarly, an examination of the turbulent kinetic energy distributions at 30 L/min flow rate in Fig. 6 revealed higher energy levels in the second section. The contraction in this region increased the turbulent kinetic energy of the airflow. Unlike the velocity distributions, however, this increase persisted in subsequent sections. After gaining turbulent kinetic energy, the turbulence kinetic energy gradually dissipated until reaching the nasopharynx.

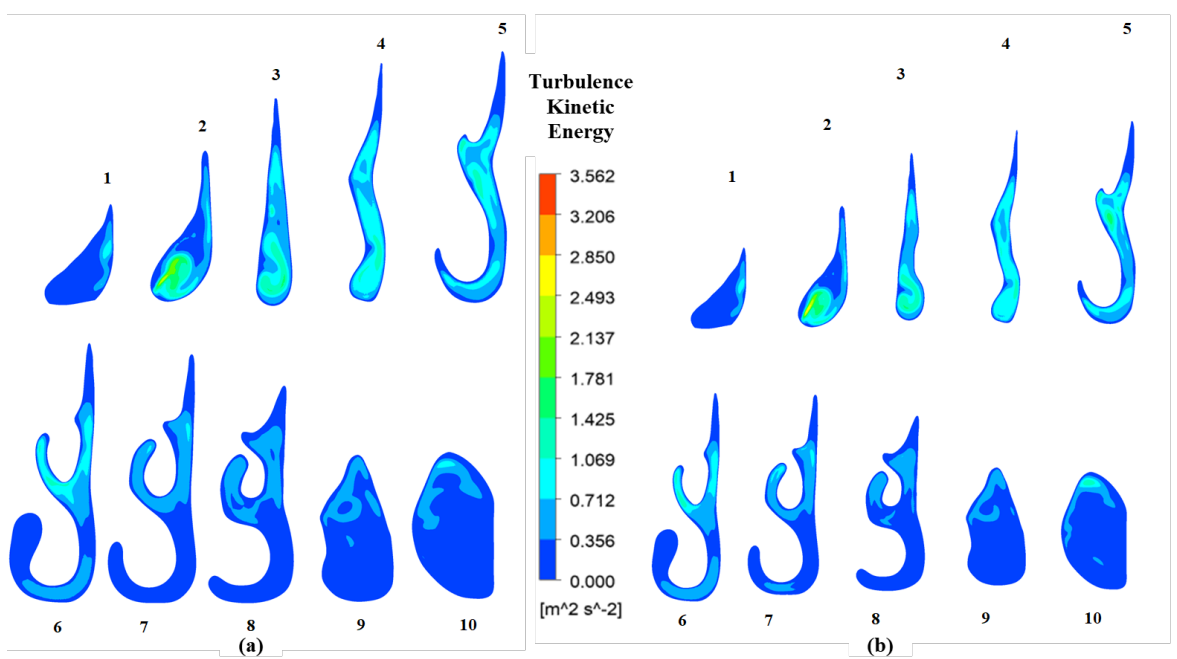


Fig. 6: Turbulent kinetic energy contours at each cross section: (a) non-deviated septum, (b) deviated septum

4. Conclusion

This study aimed to predict potential outcomes of planned treatments for nasal septal deviation through virtual septoplasty prior to actual surgery. The results demonstrate that by employing CFD analysis in this interdisciplinary approach, clinicians may preoperatively estimate how nasal resistance may change following the surgery for patients with septal deviation. While the changes in nasal resistance of post-septoplasty can be predicted by this approach, verification of positive or negative outcomes requires post-operative CT scans of actual surgical outcomes.

This methodology may assist surgeons in both developing patient-specific treatment and making evidence-based decisions about surgical necessity, potentially preventing unnecessary interventions. As an initial stage of research, this approach could evolve with technological advancements into real-time CFD analyses, possibly allowing surgeons to evaluate potential septoplasty outcomes during clinical consultations.

References

- [1] C. H. Baker, "A New Method For The Relief Of Nasal Stenosis," *Annals. of Otology, Rhinology Laryngol.*, vol. 6, no. 4, pp. 423-424, 1897.
- [2] A. W. Proetz, "Air Currents in the Upper Respiratory Tract and Their Clinical Importance," *Annals. of Otology, Rhinology Laryngol.*, vol. 60, no. 2, pp. 439-467, 1951.
- [3] Y. Liu, M. R. Johnson, E. A. Matida, S. Kherani and J. Marsan, "Creation of a standardized geometry of the human nasal cavity," *J. Appl. Physiol.*, vol. 106, pp. 784-795, 2009.
- [4] D. J. Doorly, D. J. Taylor and R. C. Schroter, "Mechanics of airflow in the human nasal airways," *Respiratory Physiol. & Neurobiol.*, vol. 163, pp. 100-110, 2008.
- [5] C. Croce, R. Fodil, M. Durand, G. Sbirlea-Apiou, G. Caillibotte, J. F. Papon, J. R. Blondeau, A. Coste, D. Isabey and B. Louis, "In Vitro Experiments and Numerical Simulations of Airflow in Realistic Nasal Airway Geometry," *Annals. of Biomedical Eng.*, vol. 34, no. 6, pp. 997-1007, 2006.
- [6] D. J. Taylor, D. J. Doorly and R. C. Schroter, "Inflow boundary profile prescription for numerical simulation of nasal airflow," *J. R. Soc. Interface*, vol. 7, pp. 515-527, 2009.

- [7] M. Zhao, T. Barber, P. Cistulli, K. Sutherland and G. Rosengarten, "Computational fluid dynamics for the assessment of upper airway response to oral appliance treatment in obstructive sleep apnea," *J. of Biomechanics*, vol. 46, pp. 142-150, 2012.
- [8] F. Chometon, P. Gillieron, J. Laurent, D. Ebbo, P. Koifman, F. Lecomte and N. Sorrel-Dejerine, "Aerodynamics of Nasal Airways with Application to Obstruction," *Int. Conf. on Fluid Control, Measurements, and Visualization*, Saskatchewan, Canada, 2000.
- [9] C. Xu, S. Sin, J. M. McDonough, J. K. Udupa, G. Allon, R. Arens and D. M. Wootton, "Computational fluid dynamics modeling of the upper airway of children with obstructive sleep apnea syndrome in steady flow," *J. of Biomechanics*, vol. 39, pp. 2043-2054, 2005.
- [10] G. Mylavarapu, M. Mihaescu, L. Fuchs, P. Georgios and E. Gutmark, "Planning human upper airway surgery using computational fluid dynamics," *J. of Biomechanics*, vol. 46, pp. 1979-1986, 2013.
- [11] T. Flint, M. Esmaily-Moghadam, A. Thamboo, N. Velasquez and P. Moin, "Computational investigation of empty nose syndrome," *Center for Turb. Res. Ann. Res. Briefs*, pp. 251-260, 2015.
- [12] M. R. Jordal, "Patient specific numerical simulation of flow in the human upper airways," M.Sc. Thesis, Dept. of Energy and Process Eng., Norwegian Univ. of Sci. Tech., Norway, 2016.
- [13] Y. Fan, L. K. Cheung, M. M. Chong, K. W. Chow and C. H. Liu, "Computational Study on Obstructive Sleep Apnea Syndrome Using Patient Specific Models," *Proceedings of the World Cong. on Eng.*, vol. 3, London, UK, 2011.
- [14] S. Kita, M. Oshima, K. Shimazaki, T. Iwai, S. Omura and T. Ono, "Computational Fluid Dynamic Study of Nasal Respiratory Function Before and After Bimaxillary Orthognathic Surgery With Bone Trimming at the Inferior Edge of the Pyriform Aperture," *American Assoc. of Oral and Maxillofacial Surg.*, vol. 74, pp. 2241-2251, 2016.
- [15] S. K. Kim, G. E. Heo, A. Seo, Y. Na and S. K. Chung, "Correlation between nasal airflow characteristics and clinical relevance of nasal septal deviation to nasal airway obstruction," *Resp. Phys. & Neurobiology*, vol. 192, pp. 95-101, 2013
- [16] G. J. Garcia, J. S. Rhee, B. E. Senior and J. S. Kimbell, "Septal deviation and nasal resistance: An investigation using virtual surgery and computational fluid dynamics," *American J. of Rhinology & Allergy*, vol. 24, no. 1, pp. 46-53, 2010.
- [17] G. Xiong, J. Zhan, K. Zuo, J. Li, L. Rong and G. Xu, "Numerical flow simulation in the post-endoscopic sinus surgery nasal cavity," *Med. Biol. Eng. Comput.*, vol. 46, pp. 1161-1167, 2008.
- [18] S. Ozlugedik, G. Nakiboglu, C. Sert, A. Elhan, E. Tonuk, S. Akyar and I. Tekdemir, "Numerical Study of the Aerodynamic Effects of Septoplasty and Partial Lateral Turbinectomy," *The Laryngoscope*, vol. 118, pp. 330-334, 2008.
- [19] J. S. Rhee, S. S. Pawar, G. J. Garcia and J. S. Kimbell, "Towards Personalized Nasal Surgery Using Computational Fluid Dynamics," *American Academy of Facial Plastic and Reconstructive Surg. Annual Meeting*, Boston, US, 2010.
- [20] T. Liu, D. Han, J. Wang, J. Tan, H. Zang, T. Wang, Y. Li and S. Cui, "Effects of septal deviation on the airflow characteristics: Using computational fluid dynamics models," *Acta Oto-Laryngologica*, vol. 132, no. 3, pp. 290-298, 2011
- [21] X. B. Chen, H. P. Lee, V. F. Chong and D. Y. Wang, "Assessment of Septal Deviation Effects on Nasal Air Flow: A Computational Fluid Dynamics Model," *The Laryngoscope*, vol. 119, pp. 1730-1736, 2009.
- [22] F. M. White, Fluid Mechanics. McGraw-Hill, New York, 2011.
- [23] Ansys, Inc., "Ansys® Academic Research, Release 15, Help System, Fluent Theory Guide," 2015.
- [24] Y. Liu, E. A. Matida, J. Gu and M. R. Johnson, "Numerical simulation of aerosol deposition in a 3-D human nasal cavity using RANS, RANS/EIM, and LES," *J. of Aerosol Sci.*, vol. 38, pp. 683-700, 2007.
- [25] Y. Liu, E. A. Matida and M. R. Johnson, "Experimental measurements and computational modeling of aerosol deposition in the Carleton-Civic standardized human nasal cavity," *J. of Aerosol Sci.*, vol. 41, pp. 569-586, 2010.
- [26] I. Weinhold and G. Mlynski, "Numerical simulation of airflow in the human nose," *Eur. Arch. Otorhinolaryngol.*, vol. 261, pp. 452-455, 2003.